

Received October 10, 2019, accepted December 18, 2019, date of publication December 31, 2019, date of current version January 9, 2020.

Digital Object Identifier 10.1109/ACCESS.2019.2963355

Online Prediction of Normal Blood Viscosity During Cardiopulmonary Bypass Using Hematocrit- and Temperature-Dependent Model

SHIGEYUKI OKAHARA¹, (Member, IEEE), SATOSHI MIYAMOTO², ZU SOH³, (Member, IEEE), HIDESHI ITOH¹, SHINYA TAKAHASHI⁴, AND TOSHIO TSUJI³, (Member, IEEE)

¹Department of Medical Engineering, Junshin Gakuen University, Fukuoka 815-0036, Japan

²Department of Clinical Engineering, Hiroshima University Hospital, Hiroshima 734-8551, Japan

³Department of System Cybernetics, Institute of Engineering, Hiroshima University, Hiroshima 739-0046, Japan

⁴Department of Cardiovascular Surgery, Hiroshima University Hospital, Hiroshima 734-8551, Japan

Corresponding authors: Shigeyuki Okahara (okahara.s@junshin-u.ac.jp) and Toshio Tsuji (tsuji@bsys.hiroshima-u.ac.jp)

This work was supported by the Japan Society for the Promotion of Science (JSPS) KAKENHI under Grant JP19K12832.

ABSTRACT This paper proposes a mathematical model for online prediction of the hematocrit- and temperature-based normal blood viscosity during cardiopulmonary bypass (CPB). Clinical trials were performed using a previously developed continuous blood viscosity monitoring system, and continuous pressure- and flow-based instantaneous viscosity (η_e) data were collected from 40 patients subjected to mild to moderate hypothermic CPB. The hematocrit and blood temperature data corresponding to η_e were also acquired. It was found that the blood viscosity–temperature curves for the different hematocrit levels can be well fitted using linear models, with the parameters of the linear model (slopes and intersects) also exhibiting linear relationships with the hematocrit. Based on these relationships, we were able to predict the hematocrit- and temperature-based normal viscosity (η_0). To test the prediction accuracy, η_0 was compared with η_e using the leave-one-out cross-validation procedure. Furthermore, η_0 and the offline-measured viscosity (η), determined using a conventional viscometer, were compared for 20 patients subjected to mildly hypothermic CPB. η_0 and η_e —two online blood viscosity monitoring methods based on different principles—showed good agreement ($R^2 = 0.74$ and $p < 0.0001$). Moreover, η_0 and η also showed good agreement ($R^2 = 0.69$ and $p < 0.0001$). The proposed model is suitable for online prediction of the hematocrit- and temperature-based normal blood viscosity during CPB. The proposed model can function as the core of a future application for investigating the effects of blood viscosity during clinical perfusion management and facilitate detailed online blood viscosity studies.

INDEX TERMS Blood viscosity, cardiopulmonary bypass, hematocrit, oxygenator.

I. INTRODUCTION

Cardiopulmonary bypass (CPB) is a method for completely substituting the cardiorespiratory function during cardiac surgery to ensure a bloodless and motionless operating field. The blood drained from the right atrium bypasses pulmonary circulation, and is perfused for systemic circulation from the aorta after gas exchange with an oxygenator. The pump flow rate and perfusion pressure are the indices used

conventionally to ensure the appropriate supply of oxygen to the living body [1]. While the flow rate can be determined arbitrarily using a blood pump, the perfusion pressure depends on the blood flow and blood viscosity, which depend on the vascular resistance [2]. The blood viscosity during CPB is directly determined by the nonphysiologically controlled hematocrit and temperature [2], and variations in the blood viscosity because of this relationship are normal. Specifically, a decrease in the blood temperature from the normal temperature to 22 °C increases the blood viscosity by approximately 50–300% [3]. On the other hand, the effect

The associate editor coordinating the review of this manuscript and approving it for publication was Emil Jovanov.

on the blood viscosity is smaller in the 25–37 °C range [4]. During CPB, the body temperature is generally reduced to approximately 25–32 °C to protect the organs by decreasing the oxygen consumption [5]. Conventionally, hemodilution is performed to counter the resulting increase in the blood viscosity because of hypothermia and to maintain the blood flow [6], [7]. Although the acceptable level of hemodilution remains a matter of debate, several studies support the claim that a low hematocrit level can cause neuropathy and renal failure [8]–[12]. However, it remains to be clarified how increases in the blood viscosity due to hypothermia and a high hematocrit level are related to postoperative neurological complications with a decrease in microcirculation.

Previous epidemiologic studies have reported that blood hyperviscosity increases the risk of cerebral vessel and cardiovascular events [13]–[15]. Although the hematocrit, plasma viscosity, and erythrocyte sedimentation rate, which are the determinants of blood viscosity, reportedly exhibit independent risks with respect to cardiovascular events, the underlying mechanisms by which these rheological factors act remain uncertain [16]. In addition, the risk associated with changes in the temperature has not yet been clarified because the subjects in the above-mentioned studies had been kept in a state of normothermia, and the blood viscosity at the normal temperature is at the minimum.

Furthermore, CPB can lead to abnormal increases in the blood viscosity independent of the effects of the hematocrit and temperature. Blood is a nonNewtonian fluid with the characteristics of pseudoplastic fluids in that the apparent blood viscosity decreases because of the deformation of the red blood cells (RBCs) during microcirculation [17]. Hence, it is necessary to investigate the hemorheological characteristics that result in an increase in the blood viscosity during microcirculation when the RBC deformability is reduced [18]. When blood is exposed to mechanical stress, hypothermia, and plasma dilution, the shape of the RBCs changes [19], [20]. This may also affect RBC deformability during CPB [21]. It is also known that the decreases observed in the deformability of stored erythrocytes are related to the storage duration [22]. Moreover, patients who undergo transfusion with stored RBCs older than 7 days may exhibit an increase in flow resistance during microcirculation [23], [24]. In addition, the reduction in the RBC deformability further decreases tissue perfusion owing to hypothermia [25]. Therefore, it is important to comprehensively investigate the effects of blood viscosity in patients undergoing CPB. However, these effects remain unknown because of a lack of suitable technologies that can help determine the causes of the variations in viscosity.

We previously developed a continuous blood viscosity monitoring system based on the pressure–flow characteristics of the oxygenator. Moreover, we demonstrated that the viscosity measured using the system is in good agreement with that measured using a conventional torsional oscillation viscometer [26],[27]. However, because the developed system estimates the blood viscosity based on physical variables,

it remains unclear whether the variations in the viscosity are related to the hematocrit and temperature, or to other factors. In the present paper, by quantifying the physiological relationships between the blood viscosity and the hematocrit and temperature, we show that the blood viscosity in the normal state can be expressed as a function of these two variables. Further, we model the dependence of the blood viscosity variations during CPB with respect to the hematocrit and blood temperature to predict the normal blood viscosity in real time.

II. METHODS

This section describes the experimental procedures for deriving the online blood viscosity prediction model and for evaluating the model. The abovementioned continuous blood viscosity monitoring system [27] was used in a clinical setting to obtain online blood viscosity, hematocrit, and blood temperature data. The normal viscosity (η_0) predicted using the proposed model based on the temperature and hematocrit was compared with the instantaneous viscosity (η_e) estimated using the system based on the pressure and flow. Subsequently, η_0 was compared with the viscosity (η) measured offline using a torsional oscillation viscometer. All the tests performed on the human participants were in keeping with the principles of the Declaration of Helsinki. In addition, all the procedures used in this study were approved by the Ethical Committee of Hiroshima University (1172). Finally, all the data shown are presented as the mean \pm standard deviation. Statistical analysis was performed using the software XLSTAT (Addinsoft Inc., Paris, France) and MATLAB (The MathWorks, Inc., Massachusetts, USA). The analyses performed included the t-test, chi-square test, histogram analysis, regression analysis, and Bland–Altman plotting. Statistical significance was assumed when $p < 0.05$.

A. MEASUREMENT SYSTEM

The oxygenator (CAPIOX-FX15; Terumo Cardiovascular Systems Corp., Tokyo, Japan), a venous reservoir (CX-RR40; Terumo Cardiovascular Systems Corp.), and a centrifugal pump (MP-23; Senko Medical Instrument Mfg. Co., Ltd., Tokyo, Japan) were connected using 3/8-inch polyvinyl chloride tubing to form a standard open circuit. These components comprised the clinical system, as shown in Fig. 1. The oxygenator's purge line was closed during CPB, in keeping with the recommendation of the manufacturer of the FX15 oxygenator. A three-way stopcock was attached to the inlet tube and the oxygenator outlet, and the pressure was measured at the stopcock using a transducer (DTCL03; Argon Medical Devices Japan, Inc., Tokyo, Japan). An ultrasonic blood flowmeter (Transonic[®] XL; Transonic Systems, Inc., NY, USA) was installed on the tube exiting the oxygenator. A heat exchanger was connected to the oxygenator, and the temperature was measured at the oxygenator outlet. The in-out pressures, flow, and temperature of the oxygenator were displayed on a heart lung machine (HLM) (HAS-2; Senko Medical Instrument Mfg. Co. Ltd.). To perform

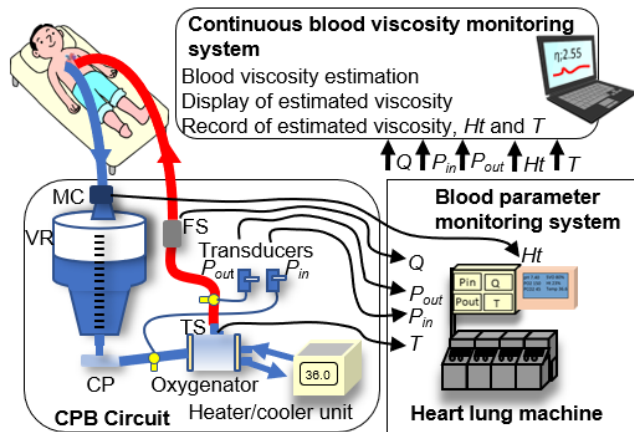


FIGURE 1. Overview of CPB circuit and system. MC: measurement cuvette; VR: venous reservoir; CP: centrifugal pump; TS: thermal sensor; FS: flow sensor; P_{in} : inlet pressure; P_{out} : outlet pressure; Q : blood flow; T : temperature; Ht : hematocrit.

selective cerebral perfusion (SCP), two cerebral perfusion lines were branched after the ultrasonic flowmeter in the main circuit and mounted onto roller pumps. The inlet pressure ($P_{in}(\tau)$), outlet pressure ($P_{out}(\tau)$), blood flow ($Q(\tau)$), and blood temperature ($T(\tau)$) of the oxygenator were output to the continuous blood viscosity monitoring system through the Universal Serial Bus (USB) port of the HLM; the sampling time, $\Delta\tau$, used was 0.5 s.

In addition, a blood parameter monitoring system (CDI-500; Terumo Cardiovascular Systems Corp.) was used for the continuous measurement of the hematocrit [28]. A cuvette for measuring the hematocrit was installed on the venous line; this ensured accurate measurements with a minimum flow rate of 0.5 L/min. The initial calibration was performed using hematocrit values measured with a hematology analyzer (MEK-6500; Nihon Kohden Co., Ltd., Tokyo, Japan) immediately after establishing a total CPB. Moreover, calibration was repeated after approximately every 30 min. The hematocrit data obtained using the CDI-500 system were sent to a personal computer every 6.0 s via a USB converter using an RS232C port.

In this study, the blood viscosities, η_e and η_0 , were determined from the data obtained with the systems described above using two different models; namely, the pressure- and flow-based viscosity model, and the hematocrit- and temperature-based viscosity model.

B. PRESSURE- AND FLOW-BASED VISCOSITY MODEL FOR CONTINUOUS BLOOD VISCOSITY MONITORING

This section describes the pressure- and flow-based blood viscosity model as well as the viscosity estimation method that we have previously proposed [27]. The following equation describes the pressure- and flow-based blood viscosity model:

$$\begin{aligned} \Delta\hat{P}(\tau) &= P_{in}(\tau) - P_{out}(\tau) \\ &= (C_r\eta_e(\tau) + C_f)Q(\tau)^{C_b\exp(C_a\eta_e(\tau))} \end{aligned} \quad (1)$$

Here, the human blood resistance parameters are set to $C_a = -0.099$, $C_b = 1.8024$, $C_f = -4.2659$, and $C_r = 6.7443$ for the FX15 oxygenator. It should be noted that a set of parameters specific to a given oxygenator and fluid can be used to estimate the viscosity from the pressure and flow data obtained from the oxygenator regardless of the type of CPB system used (i.e., one with open-type or close-type circuits or roller and centrifugal pumps). Using the data for N samples obtained within the time window, with width $\tau - (N - 1)\Delta\tau$ and τ , the pressure- and flow-based instantaneous viscosity, $\eta_e(\tau)$, can be estimated by minimizing the following evaluation function:

$$\begin{aligned} J(\eta_e(\tau)) &= \sum_{i=0}^N \left\{ \Delta P(\tau - i\Delta\tau) - (C_r\eta_e(\tau) + C_f) \right. \\ &\quad \left. \times Q(\tau - i\Delta\tau)^{C_b\exp(C_a\eta_e(\tau))} \right\}^2 \end{aligned} \quad (2)$$

where $\Delta P(\tau - i\Delta\tau)$ and $Q(\tau - i\Delta\tau)$ are the pressure gradient ($P_{in} - P_{out}$) and blood flow of the oxygenator measured at sampling time i before the present sampling time, τ . In this study, the window width was set to 4 s ($N = 8$), and the $\eta_e(\tau)$ values, which were estimated every $\Delta\tau = 0.5$ s, were saved in a comma-separated values file.

To guarantee the accuracy of the estimated viscosity values, we defined a reliability index $\varepsilon(\tau)$, which is given by (3):

$$\begin{aligned} \varepsilon(\tau) &= \frac{\sum_{n=0}^N \Delta P(\tau - i\Delta\tau)^2}{\sum_{n=0}^N \Delta P(\tau - i\Delta\tau)^2 + \sum_{n=0}^N (\Delta P(\tau - i\Delta\tau) \Delta\hat{P}(\tau - i\Delta\tau))^2} \end{aligned} \quad (3)$$

where $\Delta\hat{P}(\tau - i\Delta\tau)$ is the estimated pressure gradient of the oxygenator as determined by substituting $\eta_e(\tau - i\Delta\tau)$ in (1). Here, a $\varepsilon(\tau)$ value of 1.00 indicates that the estimated values were accurate, whereas $\varepsilon(\tau) < 0.99$ implies the presence of instantaneous noise in the pressure measurements during CPB (i.e., owing to aortic cross-clamping and blood drainage failure). Hereafter, we do not consider the time dependency and denote $\eta_e(\tau)$ as η_e to simplify the denotation. Thus, η_e is called the pressure- and flow-based instantaneous viscosity.

C. PROPOSED HEMATOCRIT- AND TEMPERATURE-BASED VISCOSITY MODEL

This section describes the proposed temperature- and hematocrit-based viscosity model for investigating the effects of blood temperature and hematocrit on blood viscosity.

To begin with, we assumed that there exists a linear relationship between blood viscosity, η_0 , and temperature, T , which is given by the following equation:

$$\eta_0 = AT + B \quad (4)$$

Next, we assumed that the hematocrit, Ht , linearly changes parameters A and B , as described by the following equations:

$$A = aHt + b \quad (5)$$

TABLE 1. Patient attributes.

No.	Age (years)	Sex	BSA (m ²)	Diagnosis	Procedures	ECC time (min)	AC time (min)	Lowest Body T (°C)	Lowest Blood T (°C)	Lowest Ht (%)	Highest Ht (%)	Lowest η_e (mPa·s)	Highest η_e (mPa·s)	Mean η_e (mPa·s)	Trans fusion (unit)
1	74	M	1.95	AS	AVR	113	81	34.2	32.4	20	25	1.96	2.36	2.14 ± 0.08	4
2	79	M	1.71	TAA	TAR	219	179	28.2	23.2	28	35	1.79	3.47	2.88 ± 0.36	14
3	63	F	1.58	MR	MVP	107	79	33.9	33.5	24	30	2.00	2.27	2.12 ± 0.07	6
4	79	M	1.68	MR, TR, Af	MVP, TAP, MAZE	191	110	34.0	32.0	23	27	1.97	2.24	2.10 ± 0.06	no
5	76	F	1.32	AR	AVR	179	108	34.2	32.9	18	26	1.69	2.15	1.89 ± 0.11	no
6	48	F	1.46	MS, Af	MVR, MAZE	136	77	34.0	33.9	17	23	1.63	1.99	2.00 ± 0.04	no
7*	68	F	1.53	TAA, AP	AAR, CABG	227	175	34.1	29.8	20	28	1.73	2.22	1.93 ± 0.09	6
8	77	M	1.67	AS	AVR	130	74	33.9	32.9	28	37	2.16	2.74	2.56 ± 0.11	no
9	82	F	1.71	AS, Af	AVR, MAZE	159	69	34.3	33.7	21	25	1.89	2.09	2.00 ± 0.04	2
10	47	F	1.60	TAA	TAR	224	88	25.8	21.5	14	23	1.41	2.06	1.67 ± 0.17	4
11	68	M	1.78	AR, AP	AVR, CABG	94	65	34.5	33.5	24	30	2.05	2.51	2.31 ± 0.09	no
12	69	F	1.34	AS	AVR	127	85	33.9	32.2	16	20	1.63	1.89	1.79 ± 0.04	2
13	45	F	1.66	MR	MVP	197	161	34.5	33.6	19	27	1.75	2.29	2.01 ± 0.15	no
14	72	F	1.42	TR, Af	TAP, MAZE	105	39	35.3	35.1	21	27	1.88	2.21	2.05 ± 0.06	no
15	85	F	1.53	AS	AVR	100	66	34.1	32.5	21	26	1.81	2.19	2.01 ± 0.06	no
16	70	M	1.75	MR, AP	MVR, CABG	128	67	33.9	33.3	21	29	1.72	2.19	1.93 ± 0.08	4
17	68	F	1.75	AS	AVR	115	80	34.8	34.0	18	26	1.77	1.95	1.85 ± 0.03	no
18	77	M	1.69	AS	AVR	84	61	34.3	33.0	21	26	1.71	2.08	1.93 ± 0.07	no
19	76	M	1.48	AS	AVR	86	68	34.7	32.9	21	34	1.89	2.25	2.04 ± 0.08	4
20	44	M	1.96	MR	MVP	169	108	33.9	32.0	24	29	1.89	2.43	2.13 ± 0.12	no
21	43	M	1.96	AR, TAA	AVR, AAR	115	77	34.2	33.6	25	32	2.02	2.48	2.22 ± 0.08	no
22	67	M	1.71	MR, TR, Af	MVP, TAP, MAZE	184	132	35.0	33.9	23	31	1.85	2.36	2.09 ± 0.10	4
23	78	M	1.59	AS, MR, TR	AVR, MVR, TAP	170	126	34.9	33.4	24	32	1.89	2.30	2.07 ± 0.07	8
24	73	F	1.56	MR, TR	MVP, TAP	162	105	34.5	33.4	20	25	1.86	2.19	2.06 ± 0.08	6
25	75	M	1.93	AR	AVR	108	85	34.2	32.3	25	34	1.91	2.47	2.16 ± 0.11	no
26	75	M	1.66	MR	MVR	113	70	34.0	33.2	22	26	1.87	2.09	2.00 ± 0.06	4
27	65	M	1.93	MR, TR	MVR, TAP	146	96	34.1	32.8	27	32	2.06	2.55	2.26 ± 0.13	2
28	66	M	1.83	AR, Af	AVR, MAZE	104	64	34.2	33.2	27	32	2.01	2.46	2.27 ± 0.10	no
29	66	F	1.67	MR, Af	MVP, MAZE	127	76	34.4	33.8	20	31	1.72	2.21	1.97 ± 0.12	no
30	61	M	1.73	MR	MVR	141	89	33.9	33.2	25	37	1.85	2.70	2.20 ± 0.16	no
31	70	F	1.34	AS, Af	AVR, MAZE	91	61	33.7	32.7	20	24	1.82	2.10	1.95 ± 0.06	6
32	49	F	1.72	MR	MVR	122	73	34.3	32.9	20	31	1.81	2.32	2.05 ± 0.14	2
33	50	F	1.60	AR, TAA	AVR, AAR	130	91	34.2	33.3	19	24	1.76	2.02	1.88 ± 0.06	6
34	81	F	1.49	MR, TR	MVR, TAP	122	90	34.2	31.8	18	25	1.70	2.01	1.84 ± 0.06	2
35	73	M	1.50	MR	MVR	100	64	33.9	31.2	18	27	1.60	2.03	1.81 ± 0.09	12
36	87	M	1.83	TAA	TAR	200	101	27.5	21.3	23	28	1.91	2.83	2.42 ± 0.31	8
37	69	M	1.61	MR, TR	MVP, TAP	128	91	34.3	30.9	24	30	1.81	2.22	2.05 ± 0.06	no
38**	84	F	1.21	AR, TAA	AVR, AAR	94	61	34.5	33.0	22	24	1.76	1.99	1.86 ± 0.05	4
39	62	F	1.47	CT	CTR, MVP, MAZE	114	55	35.5	35.1	28	34	1.96	2.29	2.09 ± 0.08	6
40**	78	M	1.66	MR, OMI	MVR, CABG	138	69	34.8	33.4	17	30	1.71	2.21	1.89 ± 0.12	8

BSA: body surface area; ECC: extracorporeal circulation; AC: aortic cross-clamp; T: temperature; Ht: hematocrit; η_e : blood viscosity using continuous blood viscosity monitoring system; AS: aortic stenosis; TAA: thoracic aortic aneurysm; MR: mitral regurgitation; TR: tricuspid regurgitation; Af: atrial fibrillation; MS: mitral stenosis; AR: aortic regurgitation; AP: angina pectoris; CT: cardiac tumor; OMI: old myocardial infarction; AVR: aortic valve replacement; TAR: total arch aortic replacement; MVP: mitral valvuloplasty; TAP: tricuspid annuloplasty; MAZE: maze procedure; MVR: mitral valve replacement; CABG: coronary artery bypass grafting; AAR: ascending aortic replacement; CTR: cardiac tumor resection. *Myocardial infarction, **Stroke

$$B = cHt + d \tag{6}$$

Finally, by substituting (5) and (6) into (4), we obtained (7):

$$\eta_0(T, Ht) = (aHt + b)T + (cHt + d) \tag{7}$$

Assuming that blood viscosity is normal, that is, there is no RBC deformation or aggregation, the four parameters *a*, *b*, *c*, and *d* can be determined by approximating η_e using the least-squares method. Subsequently, blood viscosity calculated using (7) is the hematocrit- and temperature-based predicted normal viscosity, η_0 .

D. CLINICAL PROCEDURES

Data obtained from 40 patients who had undergone elective cardiac surgery with CPB at Hiroshima University Hospital over a period of 24 months (April 2016 to March 2018) were analyzed. The attributes of the patients are listed in Table 1. The operative methods performed included heart valve surgery, aortic aneurysm surgery, and combined coronary artery bypass graft (CABG) surgery, during which the blood temperature and hematocrit level can vary significantly. Of the 40 patients, one experienced myocardial infarction and two experienced cerebral infarction events post operation.

For each patient, the CPB circuit, including the FX15 oxygenator and measurement systems described in Section II-A,

was used. The priming solution consisted of 500mL acetic acid Ringer solution (BICARBON; AY pharmaceuticals Inc., Tokyo, Japan), 500 mL blood plasma expander (VOLUVEN 6% solution for infusion; Fresenius Kabi Japan Inc., Tokyo, Japan), and 300 mL 20% mannitol (MANNITOL INJECTION; YOSHINDO Inc., Toyama, Japan). Acetic acid Ringer solution or 5% albumin (Albuminar 5%; CSL Behring K.K., Tokyo, Japan) was added if necessary. After median sternotomy and systemic heparinization were performed, complete CPB was established through an arterial cannula in an ascending aorta and bicaval vein cannula and maintained for an activated clotting time greater than 480 s, while ensuring anticoagulation. Three of the patients, who underwent total arch replacement (TAR) under SCP, were perfused with systemic circulation through an 8-mm artificial conduit in the right subclavian artery. During the systemic circulatory arrest for the distal aortic anastomosis, antegrade SCP was applied to the left carotid and left subclavian arteries using the cerebral perfusion lines [29]. With respect to perfusion management, systemic cooling was performed to ensure a target bladder temperature of 34 or 25 °C for TAR during aortic cross-clamping. After establishing the complete extracorporeal circulation, the perfusion pressure was changed to a mean arterial pressure of 50–80 mmHg at a perfusion flow rate of 2.2–2.5 L/min/m². The hematocrit level was controlled by

transfusion such that it was never lower than 21 %, whereas RBC concentrates were used in 23 patients (5.5 ± 3.2 units). Myocardial protection was ensured by infusing a cold blood cardioplegic solution at 10 °C every 20 min and performing warm blood hyperkalemic cardioplegia at 37 °C before aortic declamping.

E. ANALYSIS CONFIGURATIONS

1) RELATIONSHIP BETWEEN PRESSURE- AND FLOW-BASED INSTANTANEOUS VISCOSITY, HEMATOCRIT, AND TEMPERATURE

In all the cases, the pressure- and flow-based instantaneous viscosity, η_e ; reliability index, ε ; and temperature data obtained from the continuous blood viscosity monitoring system and the hematocrit data obtained from the CDI-500 system were recorded from the beginning to the end of the CPB process. The η_e and temperature data were synchronized with the hematocrit data based on the time trigger of each system. As the sampling interval for the hematocrit data was 6 s, the sampling interval for the η_e and temperature data was also changed to 6 s.

Sample exclusion was performed as defined below. The hematocrit data from the start of the CPB process to the initial calibration of the CDI-500 system and the η_e data corresponding to a reliability index, ε , of 0.98 or lower were considered unreliable and were excluded from the analysis. Furthermore, as per the manufacturer's recommendations for the CDI-500 system, the data corresponding to a blood flow rate of 0.5 L/min or lower were excluded from the analysis because of the unstable hematocrit levels in these cases. For example, in the final stage of the weaning of CPB and SCP to a single line, the flow rate in the venous line becomes lower than the blood flow.

The distributions of the hematocrit, blood temperature, and η_e over the course of the CPB process were analyzed. Next, multiple linear regression analysis was performed using η_e as the dependent variable and the hematocrit and blood temperature as the independent variables. In addition, the event group ($n = 3$) with postoperative complications was compared with the nonevent group ($n = 37$) to elucidate the relationship between the postoperative events and blood viscosity.

2) MODELING OF BLOOD VISCOSITY–TEMPERATURE RELATIONSHIP FOR EACH HEMATOCRIT LEVEL

The following data processing was performed to determine the blood viscosity characteristics dependent upon the hematocrit and blood temperature. The data for each hematocrit level (18–33% in intervals of 1%) and blood temperature (22–37 °C in intervals of 0.1 °C) was averaged to a single datapoint for each case. In other words, for the same case, if there were multiple datapoints for the same hematocrit level and blood temperature, the averaged blood viscosity value was used. Using these data, the blood viscosity–temperature relationship for each hematocrit level was modeled using

TABLE 2. Patient attributes.

Parameter	Value
AVR : MVR	13 : 7
Male : Female	11 : 9
Age (years)	72.6 \pm 10.9
BSA (m ²)	1.56 \pm 0.16
ECC (min)	165.4 \pm 47.8
ACC (min)	94.3 \pm 35.9
Lowest BT (°C)	33.7 \pm 1.54
Pre Hematocrit (%)	33.0 \pm 4.4

AVR: aortic valve replacement; MVR: mitral valve replacement; ECC: extracorporeal circulation time; ACC: aortic cross-clamp time; BSA: body surface area; BT: blood temperature.

the procedure described in Section II-C. This yielded four parameters for predicting the blood viscosity.

3) COMPARISON OF PRESSURE- AND FLOW-BASED INSTANTANEOUS VISCOSITY AND HEMATOCRIT- AND TEMPERATURE-BASED BLOOD VISCOSITY

The proposed hematocrit- and temperature-based viscosity model was validated using the leave-one-out cross-validation (LOOCV) method. First, the data for 39 of the 40 patients were used as the training data to determine the four parameters (a , b , c , and d in (7)). Subsequently, η_0 was calculated using the test data obtained from the remaining patient by substituting the determined values of the four parameters in (7). This procedure was repeated 40 times, yielding the η_0 value for 40 patients. Finally, η_0 was plotted as a function of η_e . The systematic errors and discrepancy between η_0 and η_e were assessed using Bland-Altman analysis.

4) VALIDATION OF PREDICTION ACCURACY

To test the accuracy of predictions of the proposed viscosity, η_0 , we compared η_0 with the viscosity, η , which was measured offline using a torsional oscillation viscometer. The η data used were taken from our previous report [27]. Moreover, η_0 was also calculated based on the previously offline-measured temperature and hematocrit values.

The data corresponded to 20 patients with valvular heart disease who had undergone elective cardiac surgery with CPB at Hiroshima University Hospital over a period of nine months (June 2014 to February 2015). The attributes of the patients are listed in Table 2. The CPB circuit and procedures described in Sections II-A and D were used for all the patients.

After the start of the CPB process, the blood temperature was recorded during three periods, which were chosen to represent the three thermal phases of CPB (i.e., before cooling, during stable hypothermia, and after rewarming): after the establishment of total CPB, after the aortic cross-clamping process, and after declamping. At the same time, blood samples were collected from the circuit, and the η value and hematocrit were measured using a torsional oscillation viscometer (VISCOMATE VM-10A; Sekonic Co. Ltd., Tokyo, Japan) and MEK-6500 hematology analyzer, respectively. This viscometer can measure the dynamic viscosity

TABLE 3. Multiple linear regression analysis.

Variable	B	SE B	β	CI B	p Value
Intercept	2.15	0.001	–	2.13 – 2.17	< 0.0001
Blood <i>T</i>	-0.037	0.0003	-0.356	-0.037 – -0.036	< 0.0001
Hematocrit	0.045	0.0002	0.741	0.045 – 0.046	< 0.0001
R^2	0.71				

B: nonstandardized coefficient; β : standardized coefficient; *T*: temperature; *Ht*: hematocrit; SE: standard error; CI: confidence interval.

by sensing the changes in the amplitude of the oscillations in a liquid-immersed detector, based on a constant input voltage [30]. The test sample was immediately placed in the sample cup, and the measurements were performed under static conditions. The temperature was monitored during each η measurement using sample cups placed in a water bath equilibrated to 36 °C, and the η value was recorded 10 s after the start of the measurement process.

Next, for comparison, η was plotted against the predicted η_0 . In addition, the systematic errors as well as the discrepancy between η_0 and η were assessed through a Bland-Altman analysis performed on the 60 data points (three periods for each of the $n = 20$ clinical cases).

III. RESULTS

A. ANALYSIS OF PRESSURE- AND FLOW-BASED INSTANTANEOUS VISCOSITY, HEMATOCRIT, AND TEMPERATURE DATA

The total number of datapoints corresponding to the 40 patients was 54,677. Of these, 5,978 datapoints after starting the measurement were excluded because of the poor calibration accuracy of the CDI-500 system. In addition, 416 datapoints were excluded because their corresponding reliability index, $\varepsilon(\tau)$, was low (≤ 0.98). This was because of aortic cross-clamping or declamping, and these datapoints accounted for 0.8% of the total datapoints. The number of datapoints excluded because of the blood flow level was 0.5 L/min or lower was 2,362; these accounted for 5.9 ± 2.3 min on average. Thus, the number of datapoints obtained from the 40 patients and used in the analysis was 45,921 (84% of the total number of datapoints).

Fig. 2 shows the histograms for the hematocrit, blood temperature, and blood viscosity, η_e . The results of the multiple linear regression analysis showed that there was a significant correlation between the blood viscosity, hematocrit and temperature, with $R^2 = 0.71$, and $p < 0.0001$ (see Table 3 ($n = 45,921$)). Table 4 compares the patients characteristics in the event and nonevent groups. Significant differences were observed between the lowest blood viscosity (η_e) and mean blood viscosity (η_e) values of these groups as well as between those of the patients who had undergone CABG and those who had not, with $p < 0.05$.

B. MODELING OF BLOOD VISCOSITY-TEMPERATURE RELATIONSHIP FOR EACH HEMATOCRIT LEVEL

The number of averaged datapoints from the 40 patients was 3,699. The blood viscosity–temperature relationship

TABLE 4. Patient attributes used as univariate predictors of postoperative events.

Quantity	Event (n = 3)	No event (n = 37)	p value
Age (years)	76.7 ± 8.08	67.8 ± 12.1	0.18
BSA (m ²)	1.47 ± 0.23	1.65 ± 0.18	0.29
ECC time (min)	153.0 ± 67.8	136.2 ± 37.9	0.71
AC time (min)	101.7 ± 63.6	86.8 ± 28.1	0.73
Lowest Body <i>T</i> (°C)	34.5 ± 0.35	33.7 ± 2.03	0.07
Lowest Blood <i>T</i> (°C)	30.4 ± 4.85	32.2 ± 3.19	0.59
Lowest <i>Ht</i> (%)	19.7 ± 2.52	22.0 ± 3.19	0.25
Highest <i>Ht</i> (%)	27.3 ± 3.06	28.6 ± 3.91	0.54
Lowest η_e (mPa·s)	1.73 ± 0.03	1.84 ± 0.15	0.001
Highest η_e (mPa·s)	2.14 ± 0.13	2.80 ± 3.07	0.20
Mean η_e (mPa·s)	1.89 ± 0.03	2.07 ± 0.23	0.0003
Transfusion	3 (100%)	20 (54%)	0.25
CABG	2 (67%)	2 (5%)	0.02

BSA: body surface area; ECC: extracorporeal circulation; ACC: aortic cross-clamp; *Ht*: hematocrit; *T*: temperature; η_e : blood viscosity determined using continuous blood viscosity monitoring system; CABG: coronary artery bypass grafting.

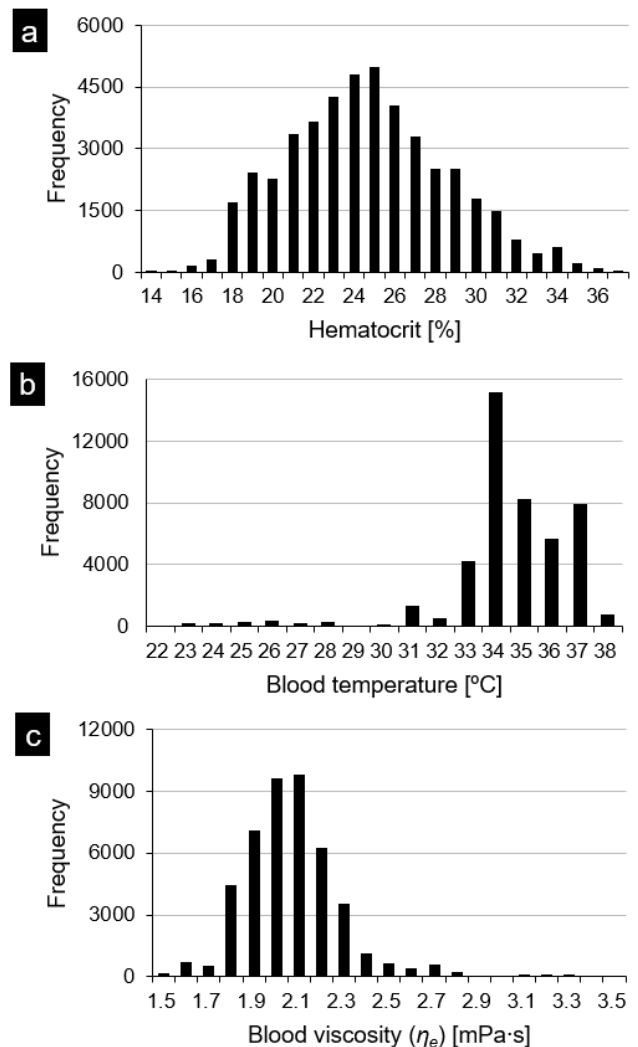


FIGURE 2. Histograms ($n = 45,921$): (a) hematocrit with bin size of 1 %, (b) blood temperature with bin size of 1 °C, and (c) blood viscosity, η_e , with bin size of 0.1 mPa·s.

characteristics for the different hematocrit levels are shown in Table 5. Linear analysis showed that, at every hematocrit level, there was a high degree of correlation between

TABLE 5. Blood viscosity-temperature relationship characteristics for each hematocrit level.

Hematocrit (%)	R^2	p value	Slope	Intercept	n
18	0.87	< 0.0001	-0.029	2.80	176
19	0.74	< 0.0001	-0.027	2.71	260
20	0.80	< 0.0001	-0.029	2.85	202
21	0.78	< 0.0001	-0.029	2.87	288
22	0.60	< 0.0001	-0.037	3.17	194
23	0.52	< 0.0001	-0.047	3.54	296
24	0.66	< 0.0001	-0.055	3.88	302
25	0.86	< 0.0001	-0.065	4.27	362
26	0.86	< 0.0001	-0.064	4.29	251
27	0.73	< 0.0001	-0.075	4.70	252
28	0.87	< 0.0001	-0.081	4.93	295
29	0.86	< 0.0001	-0.081	5.00	281
30	0.81	< 0.0001	-0.090	5.36	239
31	0.76	< 0.0001	-0.092	5.45	138
32	0.69	< 0.0001	-0.096	5.65	84
33	0.62	< 0.0001	-0.099	5.80	79

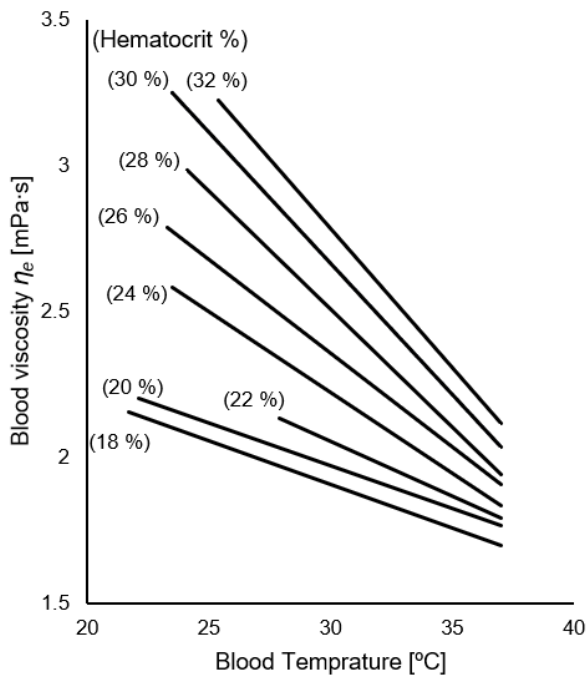


FIGURE 3. Linear fits of blood viscosity-temperature curves for various hematocrit levels.

these two parameters, with the slope of the corresponding curve being steeper at higher hematocrit levels. Some of the relationships corresponding to the characteristics in Table 5 are plotted in Fig. 3. Moreover, Fig. 4 shows the linear fitted curves for slope A and the hematocrit and intercept B and the hematocrit in (4), which represents the blood viscosity-temperature relationship. The correlation coefficient as determined from the linear approximation was 0.97 in the case of slope A and 0.98 in the case of intercept B , indicating that both parameters showed strong correlations with the hematocrit. The parameters used for predicting η_0 from Ht and T were derived from the linear approximation curves that are listed in Table 6.

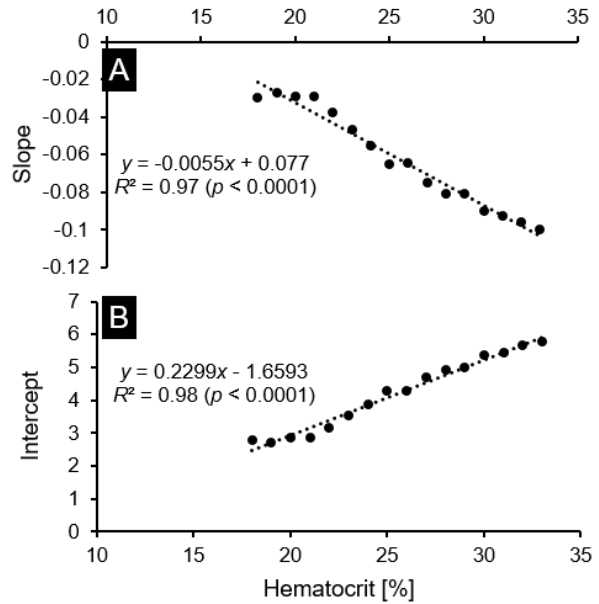


FIGURE 4. Linear curve fitting of slope (A) and intercept (B) in (4) as a function of hematocrit.

TABLE 6. Coefficients determined for (7).

Parameters	a	b	c	d
Coefficients	-0.0055	0.077	0.2299	-1.6593

C. COMPARISON OF PRESSURE- AND FLOW-BASED INSTANTANEOUS VISCOSITY, HEMATOCRIT, AND TEMPERATURE DATA

Fig. 5 shows the correlation between η_0 and η_e as determined through a LOOCV analysis. The linear regression of η_0 and η_e yielded a line with a slope of approximately 1 and a y-intercept of 0, indicating a high degree of correlation between the two parameters, with $R^2 = 0.74$ and $p < 0.0001$. Fig. 6 is the Bland-Altman analysis, which shows that the mean bias was -0.016 mPa·s, standard deviation was 0.123 mPa·s, limits of agreement were -0.257 mPa·s to 0.225 mPa·s, and error was 12.1%. No fixed bias was observed, whereas a significant proportional bias existed ($r = 0.18, p < 0.0001$). However, it did present a small-sized effect ($r = 0.18$).

D. VALIDATION OF PREDICTION ACCURACY

A comparison of η_0 and η is shown in Fig. 7. These two parameters also showed a high degree of correlation, with $R^2 = 0.69$, and $p < 0.0001$. Fig. 8 shows a result of the Bland-Altman analysis indicating a mean bias of 0.02 mPa·s, standard deviation of 0.081 mPa·s, limits of agreement of -0.139 mPa·s to 0.179 mPa·s, and error of 8.4%. Further, in this case, there was no fixed or proportion bias ($r = 0.03, p = 0.84$).

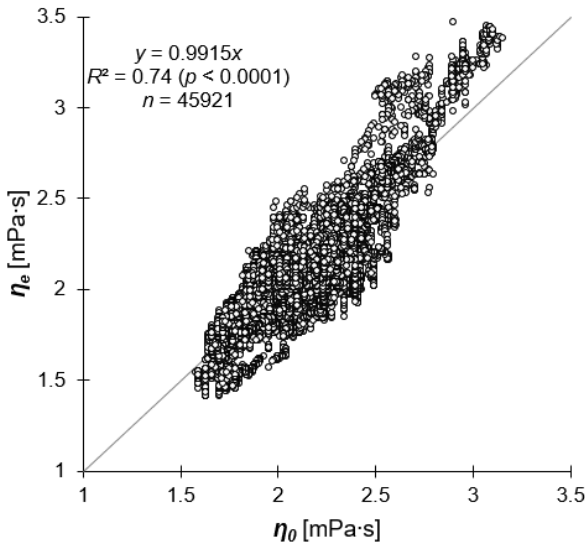


FIGURE 5. Correlations between and linear regression analysis of hematocrit- and temperature-based normal predicted viscosity (η_0) and pressure- and flow-based instantaneous viscosity (η_e). Solid line denotes line of identity.

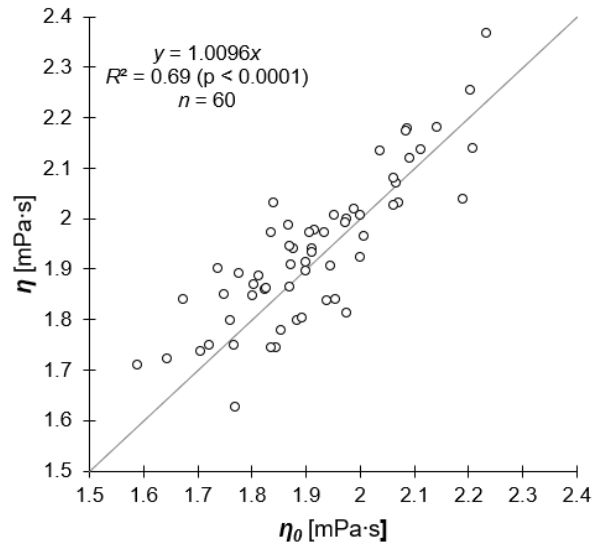


FIGURE 7. Correlation between and linear regression analysis of hematocrit- and temperature-based normal predicted viscosity (η_0) and offline-measured viscosity (η). Solid line denotes line of identity.

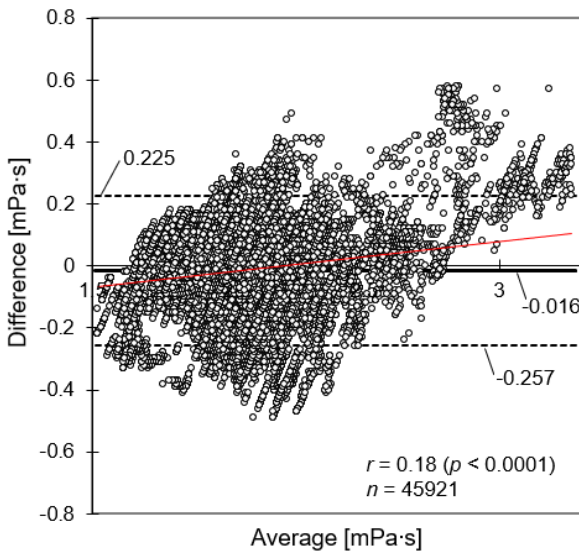


FIGURE 6. Bland-Altman plot comparing hematocrit- and temperature-based normal predicted viscosity (η_0) and pressure- and flow-based instantaneous viscosity (η_e). Solid line denotes bias (mean of difference) and dashed lines denote 95% limits of agreement (difference of two standard deviations). Red solid line represents the approximate straight line of the difference between η_0 and η_e and the mean of η_0 and η_e .

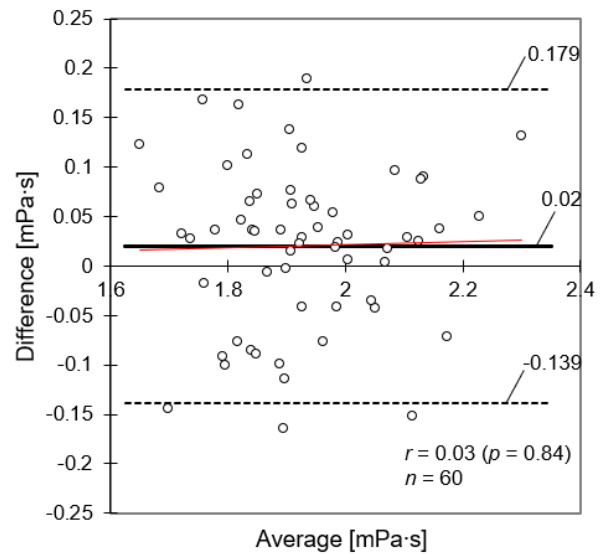


FIGURE 8. Bland-Altman plot comparing hematocrit- and temperature-based normal predicted viscosity (η_0) and offline-measured viscosity (η). Solid line denotes bias (mean of difference) and dashed lines denotes 95% limits of agreement (difference of two standard deviations). Red solid line represents the approximate straight line of the difference between η_0 and η and the mean of η_0 and η .

IV. DISCUSSION

In this study, we proposed a hematocrit- and temperature-based model of blood viscosity as well as a method for online prediction of the blood viscosity during CPB. The proposed model was validated using clinical CPB data from 40 patients with different backgrounds. The hematocrit levels were 14–37% and blood temperatures were 21–38 °C. The hematocrit values exhibited a bell-shaped distribution with a single peak corresponding to a frequency of 25%. The distribution of the blood temperature exhibited a peak in the

33–37 °C range. Further, the range of blood viscosity, η_e , was 1.4–3.5 mPa·s, and its distribution was centered in the 1.8–2.3 mPa·s range.

Unfortunately, three of the patients experienced postoperative events. It was important to know whether these events were related to their blood viscosity, to derive the parameters for predicting the normal blood viscosity based on the hematocrit and blood temperature. Further, significant differences were observed between the event and nonevent groups with respect to the lowest blood viscosity and mean blood viscosity. However, the event group exhibited lower blood viscosity

than that of the nonevent group and did not have high blood viscosity as a risk factor. Previous studies on CABG have identified the independent predictors of stroke in relation to the atherosclerosis of the ascending aorta [31]–[33]. The atherosclerosis of the ascending aorta results in an increase in the risk of microembolisms; this is because of the cannulation and cross-clamping procedures performed on the ascending aorta [34]. In this study, the CABG patients included in the event group were more likely to have splattered atherosclerotic debris because of the surgical procedure. Nevertheless, increased local blood flow owing to low blood viscosity may lead to a higher cerebral embolic load. Therefore, the relationship between the blood viscosity during CPB and any postoperative complications that arise must be investigated in the future.

The results of the multiple linear regression analysis suggested that both the hematocrit and blood temperature are significant predictors of the blood viscosity. The normal blood viscosity is determined by the hematocrit and blood temperature and, to a lesser extent, the plasma viscosity [3], while abnormal blood viscosity is induced by other phenomena related to CPB that may affect perfusion, such as hypercoagulability and deformation and aggregation of the RBCs [18], [35], [36]. Whereas these phenomena can have serious consequences, they are a rare occurrence [37]. In addition, it is known that CABG patients have, on average, higher levels of fibrinogen, which is a major determinant of the plasma viscosity [38]. We neither observed clot formation nor RBC agglutination in the devices comprising the CPB circuit for any of the patients. Furthermore, the four patients who underwent combined CABG did not have especially high viscosities.

The blood viscosity–temperature relationship was investigated for each hematocrit level. The curves, which are plotted in Fig. 3, indicated that, as the temperature decreases from 37 to 27 °C, the blood viscosity increases by a factor of 1.2 when the hematocrit is 20%, by a factor of 1.3 when the hematocrit is 26%, and by a factor of 1.5 when the hematocrit is 32%. According to a previous report by Rand *et al.* [3], the blood viscosity increases by approximately 1.2- to 1.35-fold when the normal body temperature decreases by 10 °C. In addition, the results of this study were generally consistent with those of a previous report that found that the effect of the temperature on the blood viscosity becomes more pronounced at higher hematocrit levels [3].

Although the linear regression curves for all the hematocrit levels showed some variations in terms of the coefficients of determination (lowest $R^2 = 0.52$, highest $R^2 = 0.87$), overall, they were better than the multiple regression model; i.e., the average coefficient of determination was higher. For this reason, the normal blood viscosity prediction method was derived as a nonlinear model using the blood viscosity–temperature relationships for different hematocrit levels, and the values of the four parameters in Eq. (4) were determined. Incidentally, the relationships corresponding to the hematocrit levels lower than 18% and higher than 33%

were not used to derive the parameters, as the number of corresponding samples was small. Nevertheless, the suitability of the proposed model for predicting the viscosity was confirmed by an LOOCV analysis.

Because determining the η_e value using our previously developed system [27] is the only method of performing continuous blood viscosity measurements during CPB, the algorithm for predicting η_0 was derived while assuming η_e to be the actual viscosity. Thus, in order to validate the prediction accuracy of η_0 as calculated using the parameters derived based on the estimated value, we compared it with the viscosity measured offline, η , which is the true value determined using the torsional oscillatory viscometer. The results showed that the degree of correlation between η_0 and η was similar to that between η_0 and η_e , with the accuracy also being high.

It is known that the blood viscosity can be predicted offline based on the relationship between the hematocrit and blood temperature. Eckmann *et al.* derived a mathematical expression for accurately predicting blood viscosity based on variables that describe the independent effects of the hematocrit, temperature, shear rate, and diluent on the blood viscosity [4]. However, we focused on being able to make continuous and online predictions of the blood viscosity during CPB. The primary advantage of the proposed online prediction method is that it allows one to monitor the normal blood viscosity based only on the hematocrit and blood temperature, and the effects of thrombus or the deformation and aggregation of the RBCs can be ignored. In contrast, η_e calculated with (1) using the pressure and flow data is the actual blood flow under conditions corresponding to the perfusion of the oxygenator. In the present study, we found that the two online blood viscosity monitoring methods, which are based on different principles, are comparable. Based on these findings, by continuously monitoring the ratio of η_0 to η_e , the abnormal blood viscosity levels can be evaluated while considering the effects of the hematocrit and blood temperature. In other words, a η_0/η_e ratio of 1 would indicate the normal state, whereas deviations from it would indicate an abnormal state. For example, $0 < \eta_0/\eta_e \leq 1$ may indicate an increase in the blood viscosity because of changes in the shapes of the erythrocytes.

However, we would like to make a note on the study limitations. The viscosity distributions were not normal because the proportion of hypothermia CPB cases with a body temperature of 25 °C was small. Further, the risk factors for cardiovascular and cerebrovascular events considered in this analysis were not accurately examined, given the small study size. Large-scale studies involving an analysis of the risk factors for stroke after cardiac surgery have suggested that independent risk factors such as age, history of cerebrovascular disease, urgency of operation, CPB duration of more than 2 h, high transfusion requirement, and mean arterial pressure during CPB should be considered [33], [39], [40]. Additional clinical trials are required to elucidate the risk factors related to complications in a larger population while using the blood viscosity as a risk predictor. Although the blood

viscosity characteristics dependent on the hematocrit and blood temperature reported in the present paper corresponded to a typical CPB procedure, the deep hypothermic circulatory arrest procedures used during thoracic aortic surgery decrease the blood temperature as the body temperature is lower than 20 °C. At hematocrit levels of 45% or lower, the blood viscosity changes almost linearly, whereas it increases exponentially at higher hematocrit levels [3]. Therefore, the proposed blood viscosity prediction method may not be applicable in the case of CPB procedures performed at body temperatures lower than 20 °C and hematocrit levels higher than 40%. Therefore, future investigations covering a wide range of hematocrit and blood temperature levels must be performed to demonstrate accurate predictions using nonlinear models.

V. CONCLUSION

In this study, we proposed and evaluated a model for online prediction of the normal blood viscosity during CPB based on the blood viscosity characteristics that are dependent on the hematocrit and blood temperature. First, using continuous clinical CPB data, we showed the blood viscosity-temperature relationship characteristics for each hematocrit level with a linear curve. Next, we formulated a characteristic equation that approximates normal blood viscosity from hematocrit and blood temperature data that can be obtained online. Finally, the hematocrit- and temperature-based normal viscosity predicted using the proposed model was determined to be congruent with that estimated based on the pressure and flow characteristics of the oxygenator as well as that measured offline using a conventional viscometer. Based on these results, application of the proposed model to further investigations should aid in the determination of the causes for the increases observed in blood viscosity during CPB and further assist in the management of clinical perfusion.

REFERENCES

- [1] G. S. Murphy, E. A. Hessel, and R. C. Groom, "Optimal perfusion during cardiopulmonary bypass: An evidence-based approach," *Anesthesia Analgesia*, vol. 108, no. 5, pp. 1394–1417, May 2009.
- [2] R. J. Gordon, M. Ravin, R. E. Rawitscher, and G. R. Daicoff, "Changes in arterial pressure, viscosity, and resistance during cardiopulmonary bypass," *J. Thoracic Cardiovascular Surg.*, vol. 69, no. 4, pp. 552–561, Apr. 1975.
- [3] P. W. Rand, E. Lacombe, H. E. Hunt, and W. H. Austin, "Viscosity of normal human blood under normothermic and hypothermic conditions," *J. Appl. Physiol.*, vol. 19, no. 1, pp. 117–122, Jan. 1964.
- [4] D. M. Eckmann, S. Bowers, M. Stecker, and A. T. Cheung, "Hematocrit, volume expander, temperature, and shear rate effects on blood viscosity," *Anesthesia Analgesia*, vol. 91, no. 3, pp. 539–545, Sep. 2000.
- [5] D. Machin and C. Allsager, "Principles of cardiopulmonary bypass," *Continuing Edu. Anaesthesia, Crit. Care Pain*, vol. 6, no. 5, pp. 176–181, Oct. 2006.
- [6] H. Sungurtekin, D. J. Cook, T. A. Orszulak, R. C. Daly, and C. J. Mullany, "Cerebral response to hemodilution during hypothermic cardiopulmonary bypass in adults," *Anesthesia Analgesia*, vol. 89, no. 5, pp. 1078–1083, Nov. 1999.
- [7] T. Sakamoto, G. D. Nollert, D. Zurakowski, J. Soul, L. F. Duebener, J. Sperling, M. Nagashima, G. Taylor, A. J. Duplessis, and R. A. Jonas, "Hemodilution elevates cerebral blood flow and oxygen metabolism during cardiopulmonary bypass in piglets," *Ann. Thoracic Surg.*, vol. 77, no. 5, pp. 1656–1663, May 2004.
- [8] D. Wypij, R. A. Jonas, D. C. Bellinger, P. J. Del Nido, J. E. Mayer, E. A. Bacha, J. M. Forbess, F. Pigula, P. C. Laussen, and J. W. Newburger, "The effect of hematocrit during hypothermic cardiopulmonary bypass in infant heart surgery: Results from the combined Boston hematocrit trials," *J. Thoracic Cardiovascular Surg.*, vol. 135, no. 2, pp. 355–360, Feb. 2008.
- [9] C. W. Hogue, C. A. Palin, and J. E. Arrowsmith, "Cardiopulmonary bypass management and neurologic outcomes: An evidence-based appraisal of current practices," *Anesthesia Analgesia*, vol. 103, no. 1, pp. 21–37, Jul. 2006.
- [10] G. Gravelle, "Effects of extreme hemodilution during cardiac surgery on cognitive function in the elderly," *Yearbook Anesthesiol. Pain Manage.*, vol. 2008, pp. 76–77, Jan. 2008.
- [11] R. H. Mehta, S. Castelveccchio, A. Ballotta, A. Frigiola, E. Bossone, and M. Ranucci, "Association of gender and lowest hematocrit on cardiopulmonary bypass with acute kidney injury and operative mortality in patients undergoing cardiac surgery," *Ann. Thoracic Surg.*, vol. 96, no. 1, pp. 133–140, Jul. 2013.
- [12] K. Karkouti, W. Beattie, D. Wijeyesundera, V. Rao, C. Chan, K. Dattilo, G. Djaiani, J. Ivanov, J. Karski, and T. David, "Hemodilution during cardiopulmonary bypass is an independent risk factor for acute renal failure in adult cardiac surgery," *J. Thoracic Cardiovascular Surg.*, vol. 129, no. 2, pp. 391–400, Feb. 2005.
- [13] B. M. Coull, N. Beamer, P. De Garmo, G. Sexton, F. Nordt, R. Knox, and G. V. Seaman, "Chronic blood hyperviscosity in subjects with acute stroke, transient ischemic attack, and risk factors for stroke," *Stroke*, vol. 22, no. 2, pp. 162–168, Feb. 1991.
- [14] A. J. Lee, P. I. Mowbray, G. D. Lowe, A. Rumley, F. G. R. Fowkes, and P. L. Allan, "Blood viscosity and elevated carotid intima-media thickness in men and women: The edinburgh artery study," *Circulation*, vol. 97, no. 15, pp. 1467–1473, Apr. 1998.
- [15] G. D. O. Lowe, A. J. Lee, A. Rumley, J. F. Price, and F. G. R. Fowkes, "Blood viscosity and risk of cardiovascular events: The edinburgh artery study," *Brit. J. Haematol.*, vol. 96, no. 1, pp. 168–173, Jan. 1997.
- [16] J. Danesh, "Haematocrit, viscosity, erythrocyte sedimentation rate: Meta-analyses of prospective studies of coronary heart disease," *Eur. Heart J.*, vol. 21, no. 7, pp. 515–520, Apr. 2000.
- [17] N. Maeda, "Erythrocyte rheology in microcirculation," *Jpn. J. Physiol.*, vol. 46, no. 1, pp. 1–14, 1996.
- [18] W. Reinhart and S. Chien, "Red cell rheology in stomatocyte-echinocyte transformation: Roles of cell geometry and cell shape," *Blood*, vol. 67, no. 4, pp. 1110–1118, Apr. 1986.
- [19] M. V. Kameneva, "Decrease in red blood cell deformability caused by hypothermia, hemodilution, and mechanical stress: Factors related to cardiopulmonary bypass," *ASAIO J.*, vol. 45, no. 4, pp. 307–310, Jul. 1999.
- [20] W. H. Reinhart, P. E. Ballmer, F. Rohner, P. Ott, and P. W. Straub, "The influence of extracorporeal circulation on erythrocytes and flow properties of blood," *J. Thoracic Cardiovascular Surg.*, vol. 100, no. 4, pp. 538–545, Oct. 1990.
- [21] M. Bessis, "Red cell shapes. An illustrated classification and its rationale," *Nouv. Rev. Fr. Hematol.*, vol. 12, no. 6, pp. 721–745, Nov. 1972.
- [22] P. L. Celle, "Alteration of deformability of the erythrocyte membrane in stored blood," *Transfusion*, vol. 9, no. 5, pp. 238–245, Sep. 1969.
- [23] T. L. Berezina, S. B. Zaets, C. Morgan, C. R. Spillert, M. Kamiyama, Z. Spolarics, E. A. Deitch, and G. W. Machiedo, "Influence of storage on red blood cell rheological properties," *J. Surgical Res.*, vol. 102, no. 1, pp. 6–12, Jan. 2002.
- [24] N. Z. Piety, W. H. Reinhart, P. H. Pourreau, R. Abidi, and S. S. Shevkopyas, "Shape matters: The effect of red blood cell shape on perfusion of an artificial microvascular network," *Transfusion*, vol. 56, no. 4, pp. 844–851, Apr. 2016.
- [25] T. Lecklin, S. Egginton, and G. B. Nash, "Effect of temperature on the resistance of individual red blood cells to flow through capillary-sized apertures," *Pflügers Archiv, Eur. J. Physiol.*, vol. 432, no. 5, pp. 753–759, Sep. 1996.
- [26] S. Okahara, Z. Soh, S. Miyamoto, H. Takahashi, H. Itoh, S. Takahashi, T. Sueda, and T. Tsuji, "A novel blood viscosity estimation method based on pressure-flow characteristics of an oxygenator during cardiopulmonary bypass," *Artif. Organs*, vol. 41, no. 3, pp. 262–266, Mar. 2017.
- [27] S. Okahara, Z. Soh, S. Miyamoto, H. Takahashi, S. Takahashi, T. Sueda, and T. Tsuji, "Continuous blood viscosity monitoring system for cardiopulmonary bypass applications," *IEEE Trans. Biomed. Eng.*, vol. 64, no. 7, pp. 1503–1512, Jul. 2017.

- [28] J. A. Reagor, Z. Gao, J. P. Lombardi, B. B. Millin, J. S. Tweddell, and D. S. Cooper, "Accuracy of the spectrum medical M4 and terumo CDI 500 compared to the radiometer ABL90 FLEX benchtop blood analyzer," *Perfusion*, vol. 32, no. 7, pp. 523–528, Oct. 2017.
- [29] S. Miyamoto, S. Takahashi, S. Okahara, H. Takahashi, K. Katayama, M. Watanabe, K. Maeda, S. Go, S. Morita, T. Kurosaki, B. Herlambang, and T. Sueda, "Abdominal organ protection strategy for aortic arch aneurysm surgery," *Perfusion*, vol. 33, no. 7, pp. 512–519, Oct. 2018.
- [30] V. Travagli, "Comparison of blood viscosity using a torsional oscillation viscometer and a rheometer," *Clin. Hemorheol. Microcirc.*, vol. 38, no. 2, pp. 65–74, 2008.
- [31] C. Mérie, L. Køber, P. S. Olsen, C. Andersson, J. S. Jensen, and C. Torp-Pedersen, "Risk of stroke after coronary artery bypass grafting: Effect of age and comorbidities," *Stroke*, vol. 43, no. 1, pp. 38–43, Jan. 2012.
- [32] K. Oi and H. Arai, "Stroke associated with coronary artery bypass grafting," *Gen. Thoracic Cardiovascular Surg.*, vol. 63, no. 9, pp. 487–495, Sep. 2015.
- [33] M. A. Borger, J. Ivanov, R. D. Weisel, V. Rao, and C. M. Peniston, "Stroke during coronary bypass surgery: Principal role of cerebral macroemboli," *Eur. J. Cardio-Thoracic Surg.*, vol. 19, no. 5, pp. 627–632, May 2001.
- [34] M. A. Borger, R. L. Taylor, R. D. Weisel, G. Kulkarni, M. Benarora, V. Rao, G. Cohen, L. Fedorko, and C. M. Feindel, "Decreased cerebral emboli during distal aortic arch cannulation: A randomized clinical trial," *J. Thoracic Cardiovascular Surg.*, vol. 118, no. 4, pp. 740–745, Oct. 1999.
- [35] J. W. Hoffman, T. B. Gilbert, and M. L. Hyder, "Cold agglutinins complicating repair of aortic dissection using cardiopulmonary bypass and hypothermic circulatory arrest: Case report and review," *Perfusion*, vol. 17, no. 5, pp. 391–394, Sep. 2002.
- [36] M. Blombäck, P. Kronlund, B. Åberg, K. Fatah, L.-O. Hansson, N. Egberg, E. Moor, and K. Carlsson, "Pathologic fibrin formation and cold-induced clotting of membrane oxygenators during cardiopulmonary bypass," *J. Cardiothoracic Vascular Anesthesia*, vol. 9, no. 1, pp. 34–43, Feb. 1995.
- [37] A. R. Fisher, "The incidence and cause of emergency oxygenator changeovers," *Perfusion*, vol. 14, no. 3, pp. 207–212, May 1999.
- [38] J. W. Yarnell, I. A. Baker, P. M. Sweetnam, D. Bainton, J. R. O'Brien, P. J. Whitehead, and P. C. Elwood, "Fibrinogen, viscosity, and white blood cell count are major risk factors for ischemic heart disease. The Caerphilly and Speedwell collaborative heart disease studies," *Circulation*, vol. 83, no. 3, pp. 836–844, Mar. 1991.
- [39] J. Bucnerius, J. F. Gummert, M. A. Borger, T. Walther, N. Doll, J. F. Onnasch, S. Metz, V. Falk, and F. W. Mohr, "Stroke after cardiac surgery: A risk factor analysis of 16,184 consecutive adult patients," *Ann. Thoracic Surg.*, vol. 75, no. 2, pp. 472–478, Feb. 2003.
- [40] L. Y. Sun, "Defining an intraoperative hypotension threshold in association with stroke in cardiac surgery," *Anesthesiology*, vol. 129, no. 3, pp. 440–447, Sep. 2018.



ZU SOH (Member, IEEE) received the B.E., M.E., and D.Eng. degrees in electrical and electronic engineering from Hiroshima University, Hiroshima, Japan, in 2006, 2008, and 2010, respectively.

He was a Research Fellow with the Japan Society for the Promotion of Science, from 2008 to 2013. He has been an Assistant Professor with the Department of System Cybernetics, Hiroshima University, since 2013. His current research interests include biological signal analysis, artificial life, and biological modeling.



HIDESEI ITOH received the Ph.D. degree in medical science from the Graduate School of Medicine, Dentistry and Pharmaceutical Science, Okayama University, Okayama, Japan, focus on cardiovascular surgery and emergency medicine.

He worked with Oregon Health Science University, Portland, OR, USA, from 2000 to 2001, the Kyoto Prefectural University of Medicine, Kyoto, Japan, from 2001 to 2004, the Kochi Health Sciences Center, Kochi, Japan, from 2005 to 2008, and Okayama University Hospital, Okayama, from 2008 to 2013, with Prof. S. Sano in pediatric cardiovascular surgery fields. Since 2013, he has been working as a Professor with the Department of Clinical-Bio Medical Engineering, Graduate School of Health Sciences, Junshin Gakuen University, Fukuoka, Japan. His research interests include pediatric cardiopulmonary bypass and mechanical circulatory and respiratory support.

He received the Rose Award, in 2000 from Oregon Health Science University, William Williams. MD. Young investigator awards, in 2009 from Dallas, Texas, and Best presentation awards, in 2014 from Kyoto, Williams S. Pierce. MD. Biomedical Engineering Awards, in 2015.



SHINYA TAKAHASHI received training for medical doctor, from 1992 to 1998, and graduated from Hiroshima University, Hiroshima, Japan in 1998.

He worked as a Resident of general surgery with the Hiroshima University Hospital, in 1998, and Kure Kyosai Hospital, from 1999 to 2001. He took a training for cardiovascular surgery with Kurashiki Central Hospital, from 2001 to 2004. From 2004 to 2005, he was a Clinical Fellow with the Turin University Hospital, Turin, Italy. From 2005, he worked as a Medical Staff with Hiroshima University Hospital and also the Graduate School of Biomedical and Health Science, Hiroshima University, for research of cardiovascular surgery. In 2019, he was appointed as a Professor and the Chairman, with the Graduate School of Biomedical and Health Science, Department of Surgery, Hiroshima University. Recently, his works include regeneration therapy by mesenchymal stem cells. His research interest includes graft assessment of coronary artery surgery, novel techniques of mitral valve repair, myocardial protection during cardiac arrest, spinal cord ischemia during thoracoabdominal aortic surgery, and medical device development



TOSHIO TSUJI (Member, IEEE) received the B.E. degree in industrial engineering, and the M.E. and Dr. Eng. degrees in systems engineering in 1982, 1985, and 1989, respectively, from Hiroshima University, Higashihiroshima, Japan.

He has been a Full Professor with the Department of System Cybernetics, Hiroshima University, since 2002. His research interests range from engineering to human science, with focus on cybernetics, medical electronics, computational neural sciences, and particularly biological Kansei modeling.

Dr. Tsuji has received 42 academic awards, including the IEEE 2003 King-Sun Fu Memorial Best Transactions Paper Award.



SHIGEYUKI OKAHARA (Member, IEEE) received the Dr. Eng. degree in biological systems engineering from Hiroshima University, Higashihiroshima, Japan, in 2017.

He worked with the Department of Clinical Engineering, Hiroshima University Hospital, from 1998 to 2015. He has been an Associate Professor with the Department of Medical Engineering, Junshin Gakuen University, Fukuoka, Japan, since 2015. His current research interests include biological signal analysis, bioinformation and instrumentation, and biological modeling.



SATOSHI MIYAMOTO is currently pursuing the Ph.D. degree (Hons.) with the Department of Biological Systems, Graduate School of Engineering, Hiroshima University.

He has been with the Department of Clinical Engineering, Hiroshima University Hospital, Japan, since 2004. His research interests are biological signal analysis and biological modeling.